Int. J. Heat Mass Transfer. Vol. 28, No. 3, pp. 589–601, 1985
Printed in Great Britain

0017–9310/85 $3.00 + 0.00
Pergamon Press Ltd.

Heat transfer in a two-phase thermosyphon operating with a fluid in the near critical state

U. GROSS and E. HAHNE

Institut für Thermodynamik und Wärmetechnik, Universität Stuttgart,
Postf. 80 11 40, D-7000 Stuttgart 80, F.R.G.

(*Received* 2 *February* 1984)

Abstract—The heat transfer in the heating and cooling zones of a closed thermosyphon tube has been studied experimentally. Fluid pressure ($0.8 \leqslant p/p_c < 1.0$), heat flow rate ($175 \leqslant \dot{Q} \leqslant 1975$ W) and inclination angle ($0 \leqslant \phi \leqslant 60°$) of the tube were varied. Refrigerant R115 was used as a working fluid. According to the critical specific volume, the quantity of the fluid was determined. Boiling occurs in the heating zone and condensation appears in the cooling zone. Depending on pressure, there are three regimes of boiling: nucleate boiling, nucleate boiling in a transition regime and film boiling. In the thermosyphon, there exist laminar and turbulent film condensation, respectively. Combined heat transfer in the heating and cooling zones renders an overall performance with optimal conditions at an inclination angle of about $\phi = 40°$, a small heat flow rate and pressures $0.9 < p/p_c < 1.0$ as long as no film boiling occurs.

1. INTRODUCTION

A CLOSED two-phase thermosyphon—sometimes called a 'wickless heat pipe'—is a device for heat transmission. It usually consists of a straight circular tube which is closed on both ends and filled with some fluid. This tube may be inclined or in a vertical position. Heat is supplied to the lower part (heating zone) and is removed from the upper part (cooling zone). These regions are separated by a so-called transport zone. Heat is transferred inside the tube by natural convection driven by density differences only. In subcritical states in a two-phase thermosyphon, liquid and vapour coexist and evaporation of liquid takes place in the heating zone and condensation in the cooling zone.

Many practical applications of the thermosyphon principle are reported, reaching from conservation of permafrost in arctic regions [1–4] to blade cooling in gas turbines [5–7], from application in heat exchangers [8–15], heat recovery systems [16, 17], devices for solar energy utilization [18] to the avoidance of ice upon buoys [19], bulwarks of ships [20] and streets [21, 22].

Natural convection with or without a change of phase is caused by simultaneous transfer of heat and momentum. Besides a number of other effects—like intensity of body force field, geometry of tube, heat flow rate—thermophysical properties of the fluid are of special importance. It is well known that heat transfer in a fluid near its thermodynamic critical state is very favourable, because many of the properties approach extreme values in near critical state.

E. Schmidt [23] first suggested this type of heat transport in a thermosyphon in 1939. In his experiment the tube formed a closed loop. Later Schmidt [24] and Hahne [25] carried out investigations close to the critical state with a straight thermosyphon in vertical and inclined positions using NH_3 and CO_2, respectively. With regard to temperature distribution in the transport zone they obtained quite interesting results. The closed loop arrangement was pursued in some American papers. These may be represented by the work of Tanger *et al.* [26] who confirmed the results of [23]. The latest publication of near-critical heat transfer in a thermosyphon comes from Stoyanov [27]. He used the same arrangement as Schmidt [24] and obtained similar results. In all the papers mentioned above, the effective thermal conductivity of the transport zone in a closed thermosyphon was investigated in a near-critical state; processes, however, occurring in the heating zone and cooling zone were not studied. These actually are of great importance for a straight thermosyphon. Heat transfer in the heating zone and in the cooling zone of a closed two-phase thermosyphon is influenced by a great number of parameters, accordingly themes of publications are widespread. Japikse [28] gives a general review up to 1973. Since that time, the number of papers has increased considerably. All the investigations were conducted at relatively low pressures—mostly near atmospheric or at pressures corresponding to ambient temperature—but critical pressure was not reached by far. In order to learn about the fluid flow inside a two-phase thermosyphon, experiments have been carried out repeatedly with an apparatus made of glass. The two-phase (liquid–vapour) flow has been observed directly [2, 19, 29–36] or it was simulated by injecting air into water [6, 37]. Clear photographs are only found in the papers of Larkin [19] and Andros [35]. A visual observation of the processes of liquid flow in the heating and in the cooling zones of a thermosyphon at high pressures and at large heat flow rates has not been

NOMENCLATURE

A	area
d	diameter
Δh_v	enthalpy of evaporation
kA	heat transfer rate
L	length
$\dot{m}$	mass flow rate
p	pressure
$\dot{Q}$	heat flow rate
$\dot{q}$	heat flux
Re	Reynolds number
r	radius
s	thickness of a wall
U	voltage
V	volume
$\dot{V}$	volume flow rate
v	specific volume
w	velocity.

Greek symbols

α	heat-transfer coefficient
δ	thickness of a film
η	dynamic viscosity
ϑ	temperature
λ	thermal conductivity
ν	kinematic viscosity
π	relative pressure, p/p_c
σ	surface tension
τ	shear stress
ϕ	angle of inclination.

Subscripts

c	critical
CZ	cooling zone
HZ	heating zone
i	inner
l	lower side
liq	liquid
ref	reference
st	steel
TZ	transport zone
u	upper side
vap	vapour
$''$	saturated vapour
$\bar{}$	mean value.

conducted. It is hampered by high pressures, large temperature differences and differences in surface characteristics between glass and metal.

Heat transport in a thermosyphon is described by means of heat-transfer coefficients for the heating and cooling zones. In case of a vertical tube, measured condensation heat-transfer coefficients are usually compared with Nusselt's theory [2, 15, 19, 34–35, 38–41]. At low filling rates, evaporation from a falling film occurs in the heating zone. Experimental results are compared with theories analogous to Nusselt's film theory [6, 40, 42, 43]. At large filling rates, there is a two-phase mixture in the heating zone. A comparison of mean heat-transfer coefficients with pool boiling correlations mostly fails [19, 32, 44, 45], as the cavities inside the tube are incomparably small.

Since the description of the heat-transport mechanism inside a closed two-phase thermosyphon by theoretically based equations proved to be unsatisfactory, many authors presented empirical correlations [2, 29, 32, 34, 40, 42, 46, 47] which are applicable within quite narrow boundaries excluding high pressures. Investigations are concerned with the geometry of the thermosyphon tube, with the kind and filling rate of working fluids, pressures, temperatures and heat flow rates. The majority of experiments has been conducted in a vertical tube, inclination effects were of little interest.

The present investigation deals with the effects of fluid pressure, heat flow rate and inclination angle on heat transfer mechanisms inside a closed thermosyphon filled with a fluid in the near critical state.

2. EXPERIMENTS

2.1. *Experimental apparatus*

Figure 1 shows the experimental apparatus with its principal item, the thermosyphon, made of a straight circular steel tube (RSt 37) which is closed on both ends. In its lower part (heating zone), the steel tube is surrounded by a copper cylinder ($s = 15$ mm) with 12 electric heating elements imbedded in an axial direction, equally spaced around the perimeter and supplied by direct current in parallel. In the upper part (cooling zone) the steel tube, again with a copper cylinder, is surrounded by an annulus in which water flows upwards in axial direction with a maximum temperature rise of 0.3 K. Heating and cooling zones are separated from each other by the so-called transport zone. The whole thermosyphon is well insulated and swivel-mounted in a frame. The angle of inclination with respect to the vertical may be varied between $\phi = 0°$ (vertical) and $\phi = 90°$ (horizontal). Details of the apparatus are given in Table 1.

Table 1. Data of experimental apparatus

Length of heating zone	$L_{HZ} = 501$ mm
Length of transport zone	$L_{TZ} = 746$ mm
Length of cooling zone	$L_{CZ} = 765$ mm
Inner diameter of the tube	$d_i = 40$ mm
Thickness of the wall	$s = 2$ mm
Inner volume	$V = 2.514 \times 10^{-3}$ m^3
Area of heating zone ($\pi d_i L_{HZ}$)	$A_{HZ} = 0.06296$ m^2
Area of cooling zone ($\pi d_i L_{CZ}$)	$A_{CZ} = 0.09613$ m^2
Thermal conductivity of steel tube	$\lambda_{st} = 50$ W K^{-1} m^{-1}

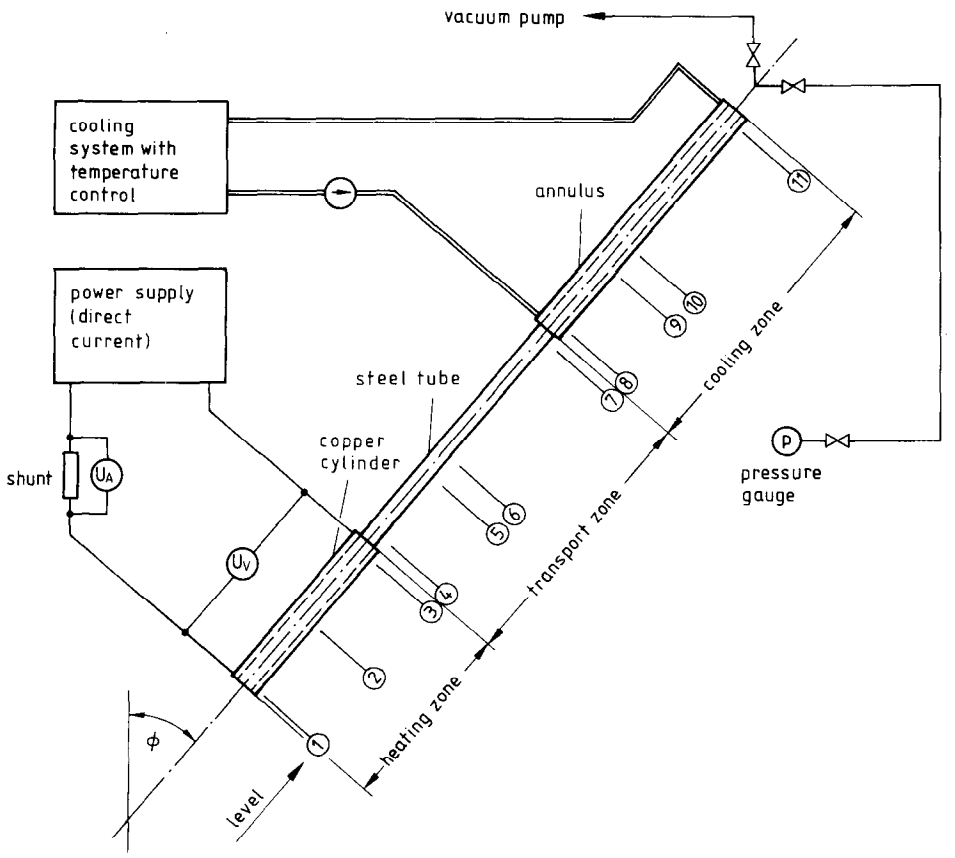

FIG. 1. Experimental apparatus.

2.2. *Working fluid*

As working fluid refrigerant R115 (Pentafluoromonochlorethane, C_2ClF_5) was used:

$$p_c = 31.258 \text{ bar} \quad \vartheta_c = 80.0°C$$

$$v_c = 1.691 \times 10^{-3} \text{ m}^3 \times \text{kg}^{-1}.$$

Two phases coexist in the subcritical state: the lower part of the tube is filled with liquid, the upper part contains vapour. The amount of fluid m is chosen for a mean specific volume which corresponds exactly to the critical value $v_c = V/m$. Thus, it is possible to reach simultaneously critical pressure and critical temperature in the fluid; the volume fraction of the liquid in the thermosyphon is about 45% and almost independent from pressure [48].

2.3. *Measurement and evaluation*

For the evaluation of the experiments, electric power, temperatures of the tube wall, pressure of the fluid and ambient pressure and temperature have to be measured.

The electric power is obtained from the direct current and voltage. The voltage U_V is measured directly at the heating elements, the current can be taken from the voltage drop U_A at the shunt (Fig. 1). The calculated electric power has to be corrected by two factors considering electric losses in the connections to the power source and heat losses through the insulation to the environment.

Wall temperatures are measured at 66 locations (Fig. 1): in 11 levels respectively six thermocouples are welded at equal intervals around the outer surface to the steel tube: level 1–3 in the heating zone, level 8–11 in the cooling zone. Measurements from all these thermocouples are taken 10 times within 10 min. Temperatures at the inner wall surface are calculated from these data taking temporal mean values. Fluid pressure is measured by a pressure gauge mounted near the axis of the thermosyphon and connected at its upper end by a thin duct without insulation. The system pressure at the upper end of the thermosyphon is calculated from the pressure gauge reading, ambient pressure and hydrostatic corrections.

Mean heat-transfer coefficients are calculated for the heating and cooling zones, respectively, from

$$\alpha_{HZ} = \frac{\dot{Q}/A_{HZ}}{\bar{\vartheta}_{HZ} - \vartheta_{ref}} \tag{1}$$

and

$$\alpha_{CZ} = \frac{\dot{Q}/A_{CZ}}{\vartheta_{ref} - \bar{\vartheta}_{CZ}}. \tag{2}$$

$\dot{Q}$ is the heat flow rate, A_{HZ} and A_{CZ} represent the heat transfer areas, $\bar{\vartheta}_{HZ}$ and $\bar{\vartheta}_{CZ}$ are the mean temperatures

of the inner surfaces in the heating and cooling zones, respectively. The reference temperature ϑ_{ref} is chosen as the mean temperature in level 6. This level is in the adiabatic region midway between heating and cooling zones and far enough from either to avoid superheating of the boiling liquid or subcooling of the condensate.

2.4. *Parameters*

The experiments comprise systematic variations of fluid pressure, heat flow rate and angle of inclination; the geometry of the tube, the working fluid and its mass were kept constant. Table 2 gives a survey of parameters used in the test series: A 'test point' is characterized by a certain combination of fluid pressure, heat flow rate and inclination angle and is measured under steady-state conditions. 'Test series' consist of a number of test points taken at a constant heat flow rate, a constant inclination angle, but under increasing values of fluid pressure.

3. RESULTS AND DISCUSSION

Operating conditions of a thermosyphon depend upon the fluid pressure within the tube. When heat is supplied in the heating zone at subcritical pressures, the liquid starts boiling on the wall. The vapour flows upwards to the cooling zone and condenses here on the inner walls of the tube. Countercurrent to this upstreaming vapour, the condensate flows down the walls into the liquid in the lower part of the tube.

The different heat transfer mechanisms in the heating and the cooling zones suggest the following classification of investigations:

—evaporation in the heating zone.
—condensation in the cooling zone.

The mean heat-transfer coefficients α_{HZ} and α_{CZ} as obtained from equations (1) and (2) are plotted vs relative pressure $\pi = p/p_c$. Heat flow rates and inclination angles are parameters in these diagrams.

3.1. *Evaporation in the heating zone*

Results. Heat-transfer coefficients are evaluated according to equation (1). The effect of heat flow rate on α_{HZ} is presented in Fig. 2 for different angles [(a) $\phi = 0°$, (b) $\phi = 10°$, (c) $\phi = 60°$]; the effect of the inclination angle is shown for different heat flow rates [(a) $\dot{Q} =$

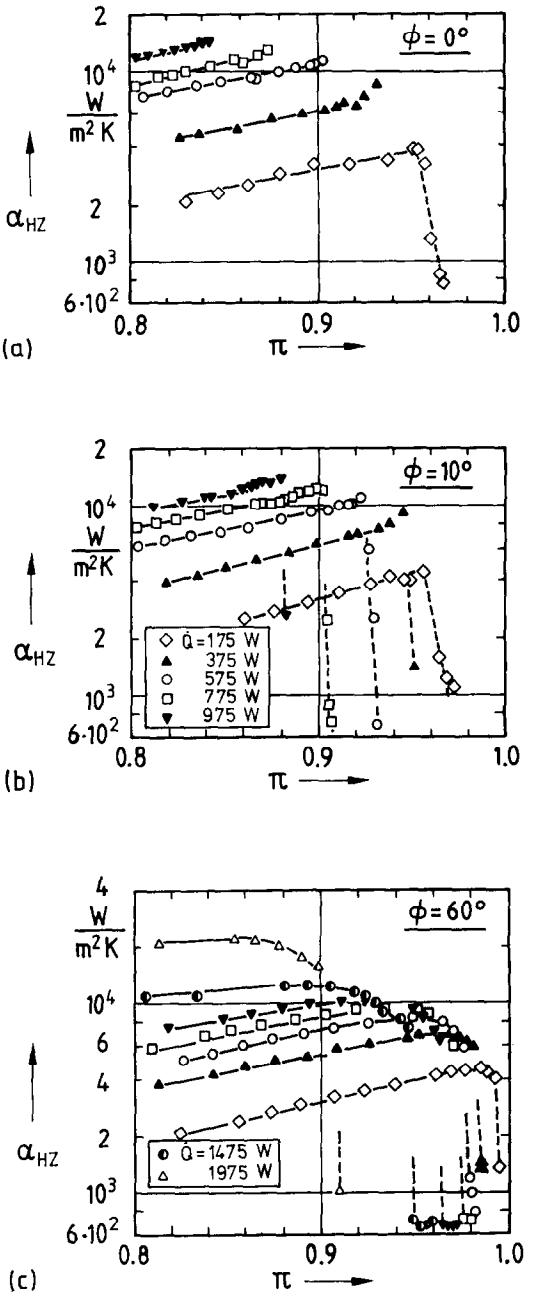

FIG. 2. Effect of the heat flow rate on the heat-transfer coefficient α_{HZ} for different inclination angles: (a) $\phi = 0°$, (b) $\phi = 10°$, (c) $\phi = 60°$.

Table 2. Parameters used in the tests

	Test series ($0.8 \leqslant \pi < 1.0$)	
	Inclination angle, ϕ (°)	Heat flow rate, $\dot{Q}$ (W)
(1) Vertical tube	0	175, 375, 575, 775, 975
(2) Small inclination angle	10	175, 375, 575, 775, 975
(3) Large inclination angle	60	175, 375, 575, 775, 975, 1475, 1975
(4) Small heat flow rate	0, 10, 20, 40, 60	375
(5) Large heat flow rate	0, 10, 20, 40, 60	775

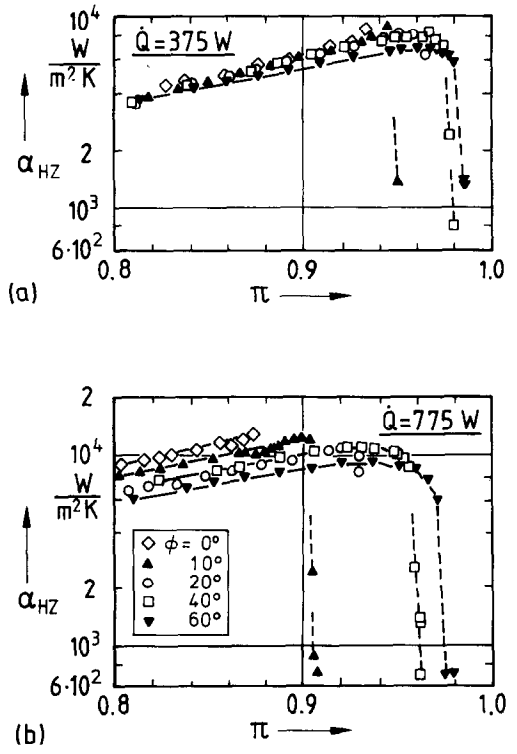

FIG. 3. Effect of the inclination angle on the heat-transfer coefficient α_{HZ} for different heat flow rates: (a) $\dot{Q}$ = 375 W, (b) $\dot{Q}$ = 775 W.

375 W, (b) $\dot{Q}$ = 775 W] in Fig. 3. Each test series is represented by points connected by a drawn-out or dashed line. Three different categories of heat-transfer coefficients can be discerned.

Category 1: large heat-transfer coefficients at the smaller pressure ratios π, with the tendency to increase when pressure and heat flow rate increase. The relation $\alpha_{HZ} \sim \dot{q}^{0.7}$ holds for large inclination angles ($\phi = 60°$), but for small angles ($\phi = 0°$) there is $\alpha_{HZ} \sim \dot{q}^{1.0}$. The effect of inclination is not very pronounced, but α_{HZ} tends to be larger for small angles (Fig. 3). For the vertical and slightly inclined (10°) tube this category ends abruptly [Figs. 2(a), 2(b)]. For tubes tilted by 60° category 1 changes over to—

Category 2: with still large heat-transfer coefficients, but now with the tendency to decrease when the pressure increases. Large heat flow rates bring the transition from category 1 into category 2 towards lower pressures [Fig. 2(c)].

Category 3: heat-transfer coefficients are smaller, by an order of magnitude, than for the other categories. For some test series with the vertical tube no heat-transfer coefficients could be obtained in this category [Fig. 2(a), e.g. for $\dot{Q} > 375$ W]. In such cases the heat transfer inside the tube became so poor that the electrically provided heat leads to temperatures too high to be handled in the test apparatus. Inclination and heat flow rate strongly affect the transition from category 2 to category 3.

The three categories of heat-transfer coefficients result from different heat transfer regimes which will be discussed in the following sections.

Nucleate boiling (regime 1). With a large enough wall superheat, nucleate boiling occurs along the heating zone. Since the thermosyphon is filled with liquid to about half its volume, the entire heating zone is flooded with liquid. Bubble frequency and bubble size depend on the thermodynamic state, e.g. the fluid saturation pressure. Driven by buoyancy, bubbles tend to rise up in the vertical direction. This motion is hindered at the upper side of the cross-section in a tilted thermosyphon, the two-phase flow has to turn into an axial direction. The situation of pure pool boiling might exist at the lower end of the tube, but in all other locations heat transfer is influenced by the superimposed two-phase flow.

Effect of pressure. This is shown in Figs. 2 and 3. The increase of heat-transfer coefficients with pressure, well known from many experiments in quite different geometries (e.g. [49, 50]) is caused by the influence of properties upon bubble nucleation and convection. If saturation temperature and pressure are raised, decreasing values of surface tension σ and enthalpy of evaporation Δh_v and a steeper boiling curve $(dp/d\vartheta)_v$ result in: (i) a rising number of active nucleation sites; (ii) a decrease of bubble size and (iii) an increase of bubble frequency. A growing bubble density—local and temporal—and a larger mass flow rate intensify microconvection in the wall boundary layer.

Effect of heat flow rate. This is shown in Fig. 2. In all cases cited, heat transfer coefficients increase with heat flow rate at constant fluid pressure—again a well known fact. An increase of heat flux results in a rise of liquid superheat near the wall and consequently to a greater number of active nucleation sites. For slightly inclined tubes the proportionality between α_{HZ} and the heat flux $\dot{q}$ is $\alpha \sim \dot{q}^{1.0}$ compared to the one common in pool boiling with $\alpha \sim \dot{q}^{0.65\ldots0.75}$. Therefore, the agreement with pool boiling results is only qualitative, the quantitative differences are probably due to the restricted space inside the thermosyphon compared to pool boiling on flat plates, on tubes and wires. The rising bubbles induce a flow in the thermosyphon with pronounced effects on heat transfer. The bubbles contain vapour of local saturation temperature while the surrounding liquid is superheated. Evaporation into the rising bubbles produces additional heat sinks in the liquid, especially in the upper parts of the heating zone where vapour accumulates.

Effect of inclination angle. This effect, shown in Fig. 3, is much less pronounced than effects of pressure and heat flow rate. Very high heat-transfer coefficients observed at small inclination angles again are caused by the two-phase flow. In the vertical tube, bubbles stream upwards outside the wall boundary layer performing as heat sinks symmetrically spread over the cross section.

In a tilted tube upstreaming bubbles are concentrated in the upper part of any cross-section. There,

heat transfer is locally improved, but it is impaired in the lower parts of a cross-section. Vapour concentration at the upper tube side increases with angle of inclination.

Nucleate boiling in transition (regime 2). The behaviour of heat-transfer coefficients here is supposed to be due to a transition regime between pure nucleate boiling (regime 1) and departure from nucleate boiling (beginning of regime 3).

For detailed investigations, the local heat-transfer coefficients at the upper and lower sides of the cross-section in levels 1, 2 and 3 of the heating zone were determined by:

$$\alpha_{HZ,u} = \frac{\dot{Q}/A_{HZ}}{\vartheta_u - \vartheta_{ref}} \tag{3}$$

and

$$\alpha_{HZ,l} = \frac{\dot{Q}/A_{HZ}}{\vartheta_l - \vartheta_{ref}}. \tag{4}$$

The analysis of $\alpha_{HZ,u}$ and $\alpha_{HZ,l}$ is restricted to a qualitative behaviour, since only the mean heat flux in the heating zone ($\dot{q} = \dot{Q}/A_{HZ}$) and not the local one could be determined. The differences in the local heat-transfer coefficients between the upper and lower sides thus appear to be smaller than they are in reality (see [48, 51]).

The local heat-transfer coefficients, equations (3) and (4), are plotted in Fig. 4 for one test series ($\phi = 60°$, $\dot{Q} = 775$ W). For lower pressure ratios, the upper side heat-transfer coefficient is larger than that on the lower side, in all three levels. The heat-transfer coefficients at the lower side of the tube increase up to high pressures (regime 1) as common for nucleate boiling and only at $\pi > 0.96$, they decrease with increasing pressure (category 2). For the upper side heat-transfer coefficients, category 2 values are obtained at different pressure ratios in the various levels.

Heat transfer at the upper side is influenced by a new effect which seems to act in level 3 at lower pressures than in levels 2 or 1. This is evident for large inclination angles. It is assumed that the reason for the decrease of the local heat-transfer coefficients is the local increase of vapour content. A continuous vapour flow may be formed in the upper part of any cross-section containing clusters of liquid which irregularly wet the wall. This would explain the observed sudden rise in the scatter of the 10 measurements taken for each of the upper side wall temperatures: from ± 0.02 K in regime 1 to ± 0.2 K in regime 2. When the pressure is raised, the volume flow rate of vapour increases for a constant heat flow rate ($\dot{V}'' = \dot{Q}v''/\Delta h_v$) with its largest value in level 3. The vapour flow in the upper part of the cross-section expands leading to a local dry-out and a decrease of $\alpha_{HZ,u}$.

The deteriorated upper side heat transfer causes a peripheral diversion of the heat flow in the tube wall towards the lower side. The values for $\alpha_{HZ,l}$ as evaluated

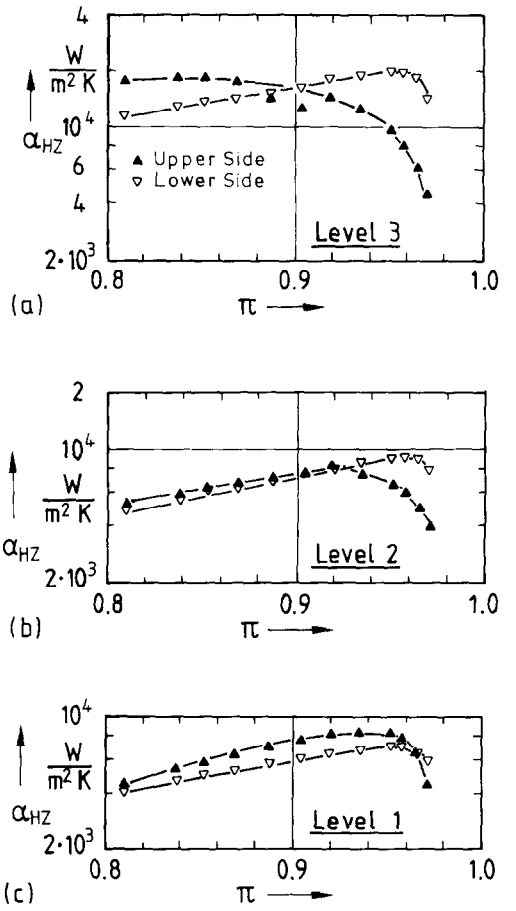

FIG. 4. Local heat-transfer coefficients α_{HZ} at the upper side and lower side of three levels ($\dot{Q} = 775$ W, $\phi = 60°$).

by equation (4) are too small in this case ($\dot{q}_l > \dot{Q}/A_{HZ}$) and it might well be that there is no decrease in $\alpha_{HZ,l}$.

Departure from nucleate boiling (regime 3). The departure from nucleate boiling is connected with a sudden drop of the heat-transfer coefficients (see Figs. 2 and 3). In all the experiments, an extraordinary increase in temperature is first observed on the upper tube side in levels 2 or 3 and this moves to the lower side within a few minutes. The transition from nucleate to film boiling is caused by a breakdown of the local fluid flow connected with the departure of vapour bubbles and the supply of liquid to the heating surface. Bubbles coalesce before they are able to escape and they form a vapour film between the wall and the liquid. This breakdown starts at locations where the mechanism of nucleate boiling is most strongly impeded. Vapour content as well as heat flux have a maximum at the upper side of the cross section in levels 2 or 3. In the transition regime a small area of poor heat transfer (vapour flow) has been established within the tube at the upper side. Adjoining this area, the nucleation mechanism is still in function bringing forward good heat transfer supported by high vapour content in the two-phase flow. This is connected with a non-uniform peripheral temperature distri-

bution. Consequently, heat flow inside the wall is not only radial, but it contains axial or peripheral components, and the heat flux from the inner surface is no longer uniform. It increases in regions of good heat transfer and has a maximum at the border to stepwise lower heat transfer coefficients [48]. As soon as the tube wall is covered by a vapour film separating liquid from the wall, the surface temperatures start to rise. This local increase induces a chain reaction: the point of maximum heat flux shifts into the adjoining region where nucleate boiling is still providing good heat transfer. This is connected with a local increase of evaporation rate and consequently with the departure from nucleate boiling in this region, too. In this way, the front between the nucleate and film boiling moves from the upper side of the tube to the lower side. The velocity of propagation is controlled by unsteady heat conduction in the tube wall.

The departure from nucleate boiling (Fig. 2) occurs at pressures which tend to be higher when the heat flow rate is chosen smaller (this is well known from pool boiling) or when the inclination angle is larger (Fig. 3).

Comparison. In the past, boiling heat transfer in a thermosyphon has been investigated only for low pressures ($\pi < 0.5$). The results, obtained with similar filling amounts, agree qualitatively with those presented in Figs. 2 and 3, although $\pi \geqslant 0.8$: an increase of heat-transfer coefficient with pressure [12, 15, 29, 32, 42, 46] and with heat flow rate [15, 29, 32, 42, 44–46] and independence of heat transfer coefficient from inclination angle for small pressures [19, 32, 42, 47, 52]. There must be distinct differences in the behaviour of a thermosyphon working at low or at high, near critical pressures:

—The surface tension at low pressures and temperatures is higher than at the critical point (where it is zero). Thus, vapour bubbles are larger and possibly exceed the tube's cross-section. Special effects, sometimes called 'non-developed boiling' [32] are produced. Plugs are formed which may explosively escape upwards [12, 19] yielding very large heat-transfer coefficients [45]. The performance of the low pressure thermosyphon is unsteady and quite violent in such cases [12, 19].
—The densities of saturated liquid and vapour differ strongly at low pressures which yields to large differences in the volume flow rates of liquid and vapour.
—The buoyancy forces affecting the bubbles are stronger with large density differences, i.e. for low pressures.

In consequence of these effects, equations derived for low fluid pressure conditions may not hold for high pressures ($\pi \geqslant 0.8$): Empirical correlations for boiling heat transfer in a thermosyphon as offered by several authors [29, 32, 34, 40, 42, 46–47], proved to be not applicable here.

In correlations derived for pool boiling, the effect of heat flow rate is considered too little and that of pressure too much. Correlations provided for boiling in forced convection are not applicable here as there is no information on vapour content and flow pattern. There is only one single paper by Savchenkov *et al.* [37] concerned with investigations dealing with these parameters in a thermosyphon, but at present, there is no possibility to give a correlation.

3.2. *Condensation in the cooling zone*

Results. Heat-transfer coefficients are evaluated according to equation (2). The effect of heat flow rate on α_{CZ} is presented in Fig. 5 for a vertical tube and in Fig. 6 for different angles [(a) $\phi = 10°$, (b) and (c) $\phi = 60°$], the effect of the inclination angle is shown in Fig. 7 for different heat flow rates [(a) $\dot{Q} = 375$ W, (b) $\dot{Q} = 775$ W].

The coefficient α_{CZ} increases with pressure. For the effect of heat flow rate, again different regimes must be distinguished. The heat-transfer coefficient decreases with increasing heat flow rates for the lower $\dot{Q}$s, but it increases for the higher $\dot{Q}$s (Figs. 5 and 6). The transition from the first regime to the second one occurs at heat flow rates which are lower for higher pressures and for smaller inclination angles.

The effect of inclination angle has to be differentiated, too: for a small heat flow rate [Fig. 7(a)], α_{CZ} increases if the angle is raised from $\phi = 0°$, it passes through a maximum at about $\phi = 40°$ and decreases again for larger angles. For the larger heat flow rates [Fig. 7(b)] a similar characteristic appears, the maximum for small pressures is also found at about $\phi = 40°$, for high pressures at $\phi = 20°$.

Vertical thermosyphon. Upstreaming vapour condenses in the cooling zone at the inner tube surface in form of a film which flows down the tube. This film is very thin at the upper end of the cooling zone, but becomes thicker on its way as further condensation occurs. Shape, thickness and velocity of the film are governed by a balance of body forces, viscosity and possibly a shear stress impressed upon the film surface.

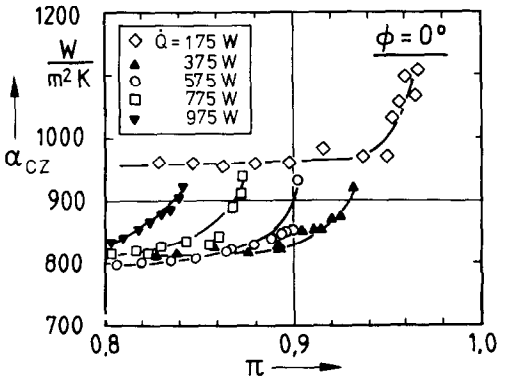

FIG. 5. Effect of the heat flow rate on the heat-transfer coefficient α_{CZ} in a vertical thermosyphon.

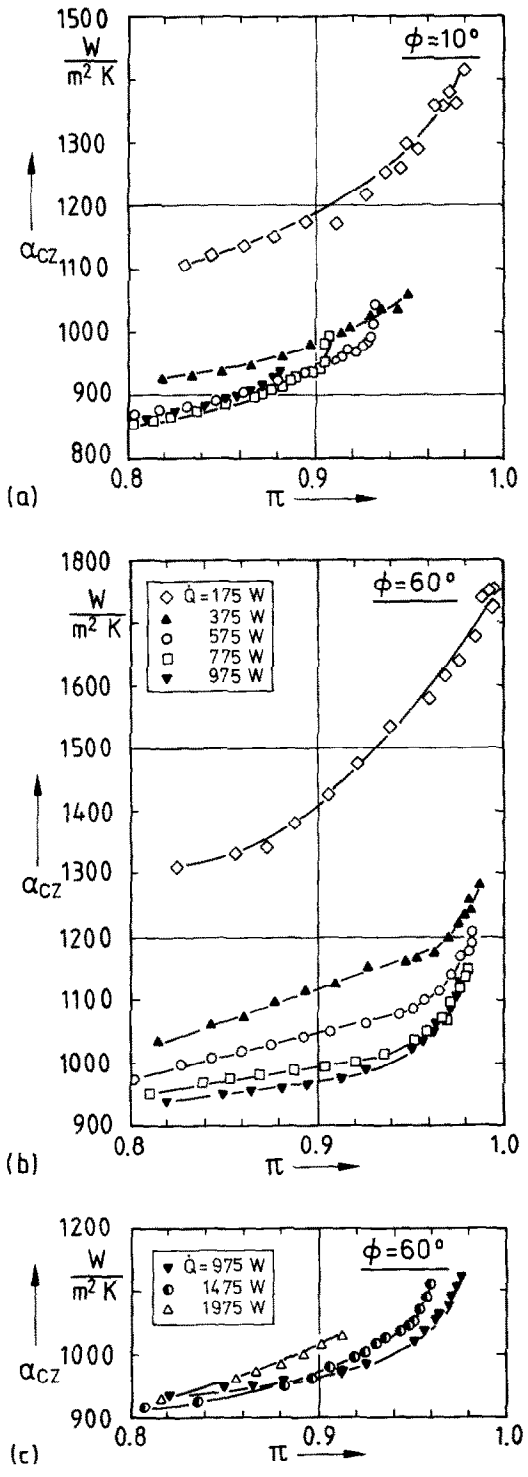

FIG. 6. Effect of the heat flow rate on the heat-transfer coefficient α_{CZ} for different inclination angles: (a) $\phi = 10°$, (b) and (c) $\phi = 60°$.

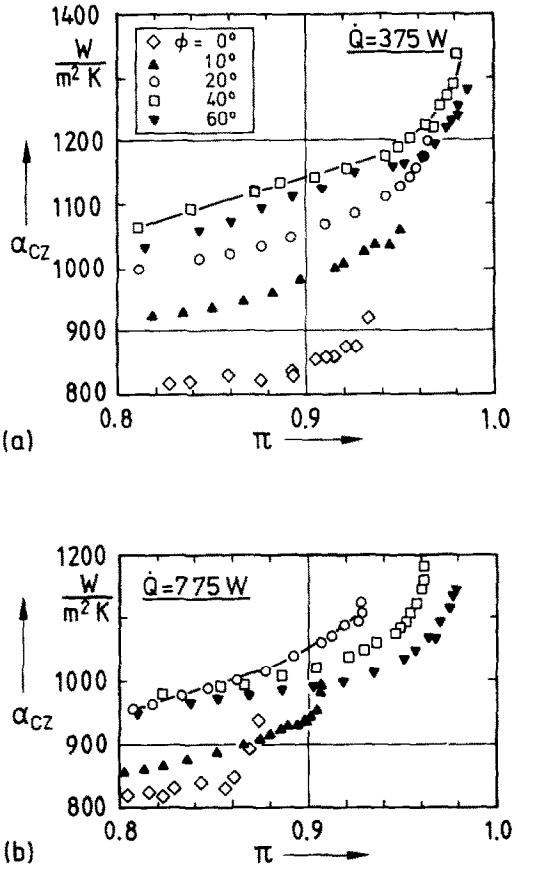

FIG. 7. Effect of the inclination angle on the heat-transfer coefficient α_{CZ} for different heat flow rates: (a) $\dot{Q} = 375$ W, (b) $\dot{Q} = 775$ W.

Flow patterns of the film may be described by means of a film Reynolds number. In the upper part of the tube the film is laminar. It will become turbulent if a certain Reynolds number is exceeded. Quite different values are mentioned in literature for this Re number ranging from 300 to 800 based on the following definition:

$$Re = \frac{\delta w}{\nu_{liq}} = \frac{\dot{Q}}{\pi d_i \eta_{liq} \Delta h_v}. \tag{5}$$

A survey of liquid flow in thin films is given by e.g. Fulford [54].

The film condensation heat transfer on a vertical surface was intensively investigated in the past. The classical works for the laminar case come from Nusselt [55] and for the turbulent film from Grigull [56].

With a rising film Re, the heat-transfer coefficients decrease in the laminar region and increase again in the turbulent region. This can be seen from Fig. 5. For a given pressure, the heat-transfer coefficient at first decreases when the heat flow rate is increased.

The condensate mass flow rate increases with the heat flow rate (and also with pressure) $\dot{m} = \dot{Q}/\Delta h_v$ which leads to a thicker film and a larger resistance for heat transport, thus α_{CZ} decreases. Decreasing values of the dynamic viscosity and of the enthalpy of evaporation as they are obtained with the approach to the critical state, let the condensate film become turbulent (equation 5) and α_{CZ} now increases with $\dot{Q}$.

Inclined thermosyphon. In contrast to the condensation inside a vertical tube with the film flowing in axial direction, conditions change basically in the case of an inclined tube. The flow direction of the condensate film now varies around the perimeter. A mass particle condensed at the upper side of a cross section moves on a spiral path to the lower side into a rivulet of condensate which now forms a rather thick film there. Various authors take Nusselt's assumptions and apply them to condensation on an inclined tube. Hassan and Jakob [57] were the first to suggest a correlation for such heat-transfer coefficients. Quite recently, Kamminga [58] presented a theoretical work confirming and supplementing the results of [55] and [57].

The effect of heat flow rate, angle of inclination and fluid pressure on condensation heat transfer inside an inclined thermosyphon shall be discussed in the following.

Effect of heat flow rate. This effect (Fig. 6) is the same as observed in a vertical tube. With a rising heat flow rate, α_{CZ} at first decreases and then increases at higher values of $\dot{Q}$. The transition occurs at higher heat flow rates and higher pressures if the angle of inclination is large.

Effect of inclination angle. This effect is shown in Fig. 7. The observed behaviour—first an increase of α_{CZ} if the angle is increased and then a decrease—may be explained with two effects: in the inclined tube condensate accumulates in the lower part of the cross section; consequently, on the average the rest of the cross section is covered by a thinner condensate film than in the vertical situation. An increasing inclination starting from $\phi = 0°$ augments such an accumulation which decreases the mean film thickness and increases α_{CZ}. This result is predicted in theoretical works [57, 58] and verified by experiments [59, 60].

At increased inclination angles the mean value of the gravity component parallel to the wall which tends to accelerate the film flow, decreases and consequently the mean film velocity becomes smaller. With a thinner and slower film covering the rest of the tube wall, laminar conditions there are kept up to larger mass flow rates ($\dot{m} = \dot{Q}/\Delta h_v$).

This first effect is superimposed by a second one. Condensate accumulated in the lower part of the cross section in an inclined tube, forms a relatively thick film streaming in an axial direction. The film velocity decreases with an increase in inclination, thus the film thickness consequently increases. A growing part of the cooling zone is thus covered and practically excluded from heat transfer. This second effect hinders heat transfer at large inclination angles (Fig. 7) so that, after an increase of the heat-transfer coefficient for small angles, this finally decreases for larger angles.

Effect of pressure. This effect is shown in Figs. 6 and 7. α_{CZ} increases exponentially with the pressure. This observation is in contradiction with Nusselt's theory of laminar film condensation which predicts an increase of film thickness and a decrease of α_{CZ} due to decreasing Δh_v and η_{liq} with increasing pressure. Nusselt's theory is based on a number of assumptions which are mostly satisfied here. One important postulation, however, is a smooth interface between film and vapour; this is not held for film Re greater than about $Re = 10$ [35, 54, 59]. A minimal disturbance, e.g. some roughness of the inner tube walls, may instigate wave formations in the film and this might be stimulated by the counterflow of liquid and vapour. Disturbances in the plain film surface are damped by viscosity η_{liq} and smoothed by surface tension σ which acts to minimize the interface area. When pressure is increased, η_{liq} and σ decrease and their stabilizing effect reduces. A destabilization originates additionally from the behaviour of some other properties considerably changing near the critical state.

Reduced Δh_v values at high pressures cause increasing flow rates of mass and volume inside the thermosyphon. Rising values of vapour volume flow rate and viscosity of vapour η_{vap} enlarge the surface shear stress and, jointly with reduced viscosity of liquid η_{liq}, increased velocity gradients are required in transverse direction:

$$\tau = -\eta_{vap}(dw/dr)_{vap} = -\eta_{liq}(dw/dr)_{liq}. \qquad (6)$$

All these effects add towards a dissolution of the smooth film surface. Waves and local eddies may develop and would lead to a reduction of the mean film thickness between wave crests. These effects are able to improve heat transfer when pressure is raised to high values in case of a laminar-wavy film. Near the critical state, the instability and waviness of the film surface is further increased yielding a steeper growth of α_{CZ}.

Comparison. The comparison of the present results with those from literature is difficult in many respects:

- —Condensation in a thermosyphon was investigated, so far, only at quite low pressures ($\pi < 0.5$).
- —The effect of an inclination angle on α_{CZ} has seldom been analysed.
- —None of the works dealing with condensation inside a thermosyphon goes beyond the laminar region.

Most of the authors, investigating condensation in a vertical thermosyphon tube, report good agreement with Nusselt's theory [2, 34, 38–41]. Larkin [15, 19] notes only a qualitative agreement as his calculated values were always somewhat smaller than his measured ones. The same is reported by Andros [35] and Hirshburg [61] who found increasing differences between calculation and measurement when the film Re was increased and waves formed. Good agreement with Nusselt's theory in the above mentioned works is probably a consequence of very low Re. Nusselt's assumptions are more likely to be fulfilled in this case.

The effect of inclination on α_{CZ} has only been investigated in some detail by Hirshburg [61]. In Stoyanov's experiments [27, 62] the inclination angle also has been varied, but heat was removed at the front side—so no comparison is possible. The present

investigations are confirmed to some extent by Hirshburg's work which gives an optimal angle of about $\phi = 70°$; this is larger than our optimal angles (in Fig. 7) of $\phi = 20$ and 40°. Equations proposed by Kamminga [58] represent the inclination effects quite well, but they fail partly for the influences of heat flow rate and totally for pressure. Predicted heat-transfer coefficients are always smaller than the measured ones. Grigull's correlation can predict α_{CZ} very well in cases where a turbulent film may be considered, i.e. if values of ϕ are small and those of $\dot{Q}$ and p are large. It proved to be impossible to correlate condensation heat-transfer coefficients obtained in the present work with any of the known equations, and further work has to be done.

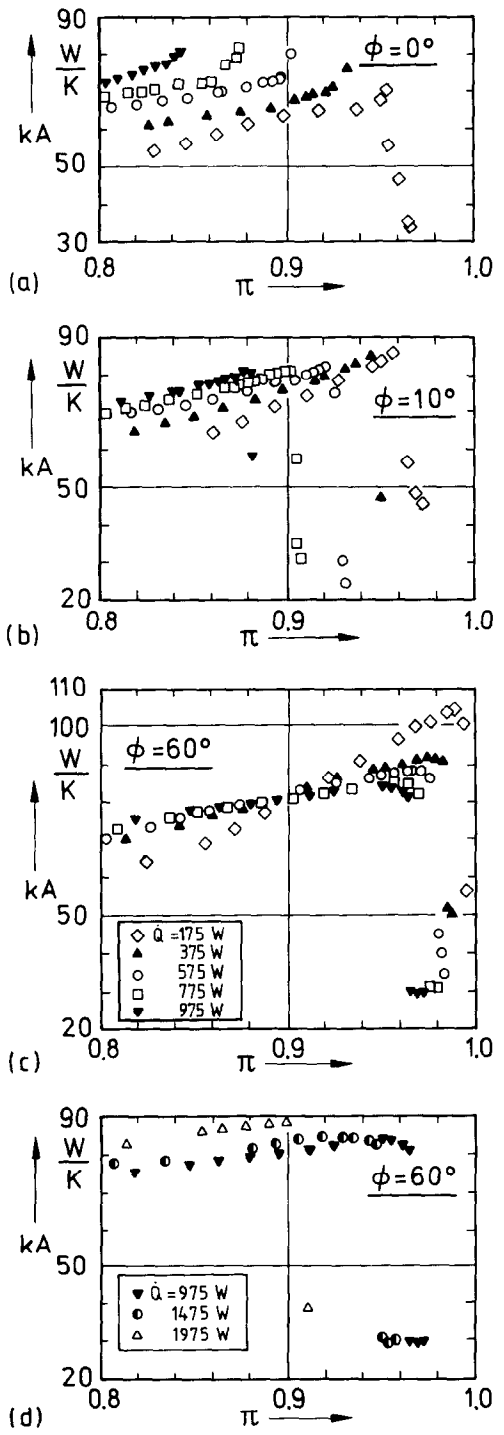

FIG. 8. Effect of the heat flow rate on the heat-transfer rate kA for different inclination angles: (a) $\phi = 0°$, (b) $\phi = 10°$, (c) and (d) $\phi = 60°$.

3.3. *Overall performance*

For the application of a thermosyphon, the singular heat transfer coefficient in particular zones is of less interest than the overall performance of the tube to transport heat. For this transport, the various heat-transfer coefficients could be combined in a conventional way to form a heat-transfer rate (kA) (or the reciprocal value of $1/kA$ as a transport resistance)

$$kA = 1\Big/\left(\frac{1}{\alpha_{HZ}A_{HZ}} + \frac{1}{\alpha_{CZ}A_{CZ}}\right). \tag{7}$$

The value of kA is governed by the smaller heat-transfer coefficient, that is α_{CZ} at lower pressures and α_{HZ} at higher ones. Results for this heat transfer rate kA are shown in Figs. 8 and 9.

The heat flow rate transported by the tube for a temperature difference $\Delta\vartheta = \bar{\vartheta}_{HZ} - \bar{\vartheta}_{CZ}$ is calculated according to

$$\dot{Q} = (kA)(\bar{\vartheta}_{HZ} - \bar{\vartheta}_{CZ}). \tag{8}$$

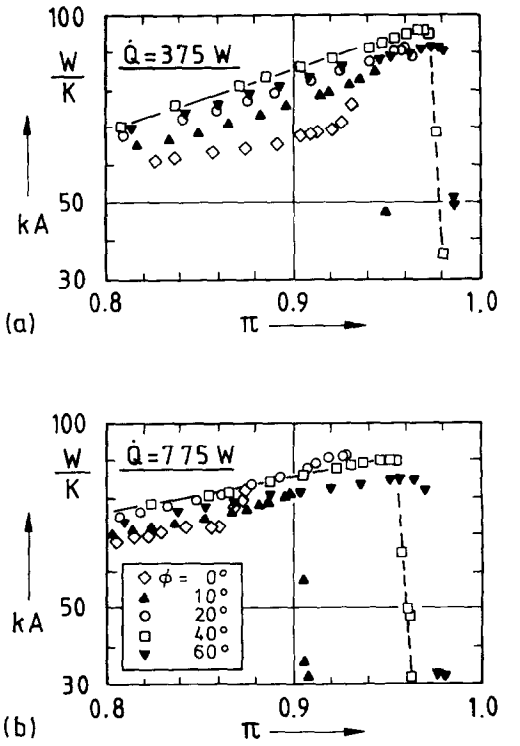

FIG. 9. Effect of the inclination angle on the heat-transfer rate kA for different heat flow rates: (a) $\dot{Q} = 375$ W, (b) $\dot{Q} = 775$ W.

4. CONCLUSIONS

Boiling and condensation processes determine the performance of a two-phase thermosyphon. The thermosyphon investigated in this work was filled with a pure fluid (R115) and operated near the thermodynamic critical state. Thus, the above mentioned processes are influenced by strong changes of the thermophysical properties of the fluid. The investigations include effects of fluid pressure and saturation temperature, effects of heat flow rate and effects of inclination angle.

In summary, the following may be concluded (Figs. 8 and 9):

—The optimum pressure for the overall performance is reached between $\pi = 0.9$ and $\pi < 1.0$. At higher pressures, departure from nucleate boiling occurs and the heat transfer rate deteriorates.
—The highest values for the heat transfer rate (kA) are obtained at either low heat flow rates (laminar condensate film) or very large ones (turbulent film).
—The optimum inclination angle is obtained at about $\phi = 40°$.

The behaviour of a thermosyphon as described here is characteristic for fluids that have:

—a low thermal conductivity in liquid state (in this work $\lambda_{liq} < 0.05$ W K^{-1} m^{-1}). The coefficient α_{CZ} becomes small for laminar film condensation.
—a low enthalpy of evaporation (in this work $\Delta h_v < 50$ kJ kg^{-1}). Then the mass flow rate inside the thermosyphon becomes quite large, especially near the critical state, yielding to a turbulent condensate film in many cases.

This characteristic is found in various refrigerants, but not in water or ammonia.

REFERENCES

1. E. L. Long, The long thermopile, *Proceedings of the Permafrost International Conference*, pp. 487–491 (1963).
2. V. V. Onosovskii, V. S. Sokolow, N. A. Buchko and Yu. N. Obraztsov, Investigation of thermopiles filled with a low-boiling liquid, *Heat Transfer—Soviet Res.* **4**, 49–55 (1972).
3. Y. Lee and U. Mital, A two-phase closed thermosyphon, *Int. J. Heat Mass Transfer* **15**, 1695–1707 (1972).
4. L. L. Vasiliev, S. L. Vaaz, L. P. Grakovich and V. M. Sedelkin, Heat transfer studies for heat pipe cooling and freezing of ground, in *Advances in Heat Pipe Technology* (edited by D. A. Reay). Pergamon Press. Oxford, pp. 63–71 (1981).
5. E. Schmidt, Wärmeübertragung durch natürliche Konvektion in starken Fliehkraftfeldern bei der Kühlung von Gasturbinen, *Abh. Braunschw. wiss.* Ges **1**, 109–115 (1949).
6. H. Cohen and F. J. Bayley, Heat-transfer problems of liquid-cooled gas-turbine blades, *Proc. Instn mech. Engrs* **169**, 1063–1080 (1955).
7. F. J. Bayley and N. Bell, Cooling turbine blades, *Engineering* **183**, 300–302 (1957).
8. N. V. Kuznetsov and A. F. Gavrilov, An airheater with an intermediate heat carrier, *Teploénergetika* **11**, 30–34 (1964).
9. A. F. Gavrilov and V. Ya. Lyakh, Air heaters with an intermediate heat carrier, *Teploénergetika* **12**, 11–17 (1965).
10. A. F. Gavrilov, Optimum parameters in an air heater with intermediate heat carrier, *Teploénergetika* **12**, 83–86 (1965).
11. A. F. Gavrilov, Design of an air heater with an intermediate heat carrier, *Teploénergetika* **13**, 92–93 (1966).
12. B. S. Larkin, Heat transfer in a two-phase thermosyphon tube, *Q. Bull. Div. mech. Engng natn Aeronaut. Establ. Can.* **3**, 45–53 (1967).
13. J. Madejski and J. Mikielewicz, Liquid fin—a new device for heat-transfer equipment, *Int. J. Heat Mass Transfer* **14**, 357–363 (1971).
14. A. Lee and A. Bedrossian, The characteristics of heat exchangers using heat pipes or thermosyphons, *Int. J. Heat Mass Transfer* **21**, 221–229 (1978).
15. B. S. Larkin, An experimental study of the temperature profiles and heat transfer coefficients in a heat pipe for a heat exchanger, in *Advances in Heat Pipe Technology* (edited by D. A. Reay). Pergamon Press, Oxford, pp. 177–191 (1981).
16. J. Unk, Ammoniak-Gravitationswärmerohre zur Wärmerückgewinnung in lüftungstechnischen Anlagen, Klima-Kälte-Heizung (Ki), pp. 304–310 (1979).
17. H. Hettwer and H. H. Bath, Heat recovery in vertical systems, in *Advances in Heat Pipe Technology* (edited by D. A. Reay). Pergamon Press, Oxford, pp. 193–199 (1981).
18. R. Bairamov and K. Toiliev, Heat pipes in solar collectors, in *Advances in Heat Pipe Technology* (edited by D. A. Reay). Pergamon Press, Oxford, pp. 47–54 (1981).
19. B. S. Larkin, An experimental study of the two-phase thermosyphon tube, *Trans. C.S.M.E.* **14**, I–VIII (1971).
20. S. Matsuda, G. Miskolczy, M. Okihara, T. Okihara, M. Kanamori and N. Hamada, Test of a horizontal heat pipe de-icing panel for use on marine vessels, *Advances in Heat Pipe Technology*, Oxford, pp. 3–10 (1981).
21. W. Hurich, Fahrbahnheizung mittels Wärmerohren, Dipolma thesis, Institut für Thermodynamik und Wärmetechnik, Universität Stuttgart (1980).
22. O. Tanaka, H. Yamakaga, T. Ogushi, M. Murakami and Y. Tanaka, Snow melting using heat pipes, in *Advances in Heat Pipe Technology* (edited by D. A. Reay). Pergamon Press, Oxford, pp. 11–23 (1981).
23. E. Schmidt, E. Eckert and U. Grigull, Wärmetransport durch Flüssigkeiten in der Nähe ihres kritischen Zustandes, Jahrbuch der deutschen Luftfahrtforschung, pp. II/53–58 (1939) and Heat transfer by liquids near the critical stall, AAF Translation No. 527, Air Materials Command, Wright Field, Dayton, Ohio (April 1946).
24. E. Schmidt, Wärmetransport durch natürliche Konvektion in Stoffen bei kritischen Zustand, *Int. J. Heat Mass Transfer* **1**, 92–101 (1960).
25. E. Hahne, Wärmetransport durch natürliche Konvektion in Medien nahe ihrem kritischen Zustand, Ph.D. thesis, Technische Hochschule München (1964) and *Int. J. Heat Mass Transfer* **8**, 481–497 (1965).
26. G. E. Tanger, J. Lytle and R. I. Vachon, Heat transfer to sulfur hexafluoride near the thermodynamic critical region in a natural-circulation loop, *J. of Heat Transfer* **90**, 37–42 (1968).
27. N. M. Stoyanov, An investigation of regularities of heat transfer in a closed evaporative thermosiphon (Russian), *Dokl. Akad. Nauk. UkrSSR* **7**, 652–656 (1967).
28. D. Japikse, Advances in thermosyphon technology, *Adv. Heat Transfer* **9**, 1–111 (1973).
29. S. P. Andreev, A study of boiling and condensation in a heat transfer element, *Inzh-fiz. Zh.* **22**, 999–1005 (1972).
30. M. K. Bezrodnyi and A. I. Beloivan, Investigation of the maximum heat-transfer capacity of closed two-phase thermosyphons, *Inzh.-fiz. Zh.* **30**, 590–597 (1976).
31. M. K. Bezrodnyi, The upper limit of maximum heat-

transfer capacity of evaporative thermosyphons, *Teploénergetika* **25,** 63–66 (1978).
32. M. G. Semena and Yu. F. Kiselev, Heat-exchange processes in the heat-supply zones of two-phase thermosyphons operating on Freons 11, 113 and 142 and on water and ethanol, *Inzh.-fiz. Zh.* **35,** 211–217 (1978).
33. M. G. Semena, Maximum heat-transfer capacity of a vertical two-phase thermal siphon, *Inzh.-fiz. Zh.* **35,** 397–403 (1978).
34. H. Imura, H. Kusuda, J. I. Ogata, T. Miyazaki and N. Sakamoto, Heat transfer in two-phase closed-type thermosyphons, *Heat Transfer Jap Res.* **8,** 41–53 (1979).
35. F. E. Andros, Heat transfer characteristics of the two-phase closed thermosyphon (wickless heat pipe) including direct flow observations. Ph.D. thesis, Arizona State University (1980).
36. M. K. Bezrodnyi, A. N. Alabovsky and S. S. Volkov, Investigation of hydrodynamic characteristics of two-phase flow in a closed thermosyphon (Russian), *Izv. VUZov, Energetika* **2,** 116–121 (1980).
37. G. A. Savchenkov, I. G. Chumak and T. Shulavsky, Natural convection of two-phase boiling mixture in the thermosyphon investigation, in *Advances in Heat Pipe Technology* (edited by D. A. Reay). Pergamon Press, Oxford, pp. 105–113 (1981).
38. Z. R. Gorbis and G. A. Savchenkov, Low temperature two-phase closed thermosyphon investigation, *Proceedings of the 2nd Heat Pipe Conference*, Bologna, pp. 37–45 (1976).
39. A. N. Alabovsky, M. K. Bezrodnyi and V. F. Moklyak, Study of vapour condensation heat-transfer in vertical thermosyphons (Russian), *Izv. VUZov Energetika* **7,** 61–67 (1979).
40. M. Shiraishi, K. Kikuchi and T. Yamanishi, Investigation of heat transfer characteristics of a two-phase closed thermosyphon, in *Advances in Heat Pipe Technology* (edited by D. A. Reay). Pergamon Press, Oxford, pp. 95–104 (1981).
41. W. K. Ho and C. L. Tien. Reflux condensation characteristics of a two-phase closed thermosyphon, in *Advances in Heat Pipe Technology* (edited by D. A. Reay). Pergamon Press, Oxford, pp. 451–458 (1981).
42. G. A. Savchenkov and Z. R. Gorbis, Boiling heat transfer in low-temperature evaporating thermosiphons, *Heat Transfer Soviet Res.* **8,** 52–56 (1976).
43. M. G. Semena and Yu. F. Kiselev, Heat exchange in the heat supply zone of two-phase thermosiphons for small degrees of filling, *Inzh.-fiz. Zh.* **35,** 690–705 (1978).
44. M. K. Bezrodnyi and D. V. Alekseenko, Boiling heat transfer in closed two-phase thermosyphons, *Heat Transfer Soviet Res.* **9,** 14–20 (1977).
45. M. K. Bezrodnyi and D. V. Alekseenko, The intensity of heat transfer in the boiling section of evaporative thermosiphons, *Teploénergetika* **24,** 83–85 (1977).
46. S. P. Andreev, Investigating heat transfer with phase transitions of liquid in a closed channel, *Teploénergetika* **19,** 88–89 (1972).
47. N. M. Stoyanov, Generalization of experimental data on heat transmission through a closed evaporative thermosiphon (Russian), *Dokl. Akad. Nauk UkrSSR* **6,** 532–535 (1967).
48. U. Groß, Der Wärmeübergang in einem geschlossenen Thermosyphon, der Fluid nahe dem thermodynamisch kritischen Zustand enthält, Ph.D. thesis, Universität Stuttgart (1983).
49. D. Gorenflo, Wärmeübergang beim Blasensieden, Filmsieden und einphasiger freier Konvektion in einem großen Druckbereich. Habilitat. Dissertation, Universität Karlsruhe (1977).
50. G. Feurstein, Der Einfluß des Druckes und der Geometrie auf den Wärmeübergang beim Behältersieden nahe dem kritischen Punkt, Ph.D. thesis, Technische Universität München (1974).
51. W. Bonn, J. Iwicki, R. Krebs, D. Steiner and E. U. Schlünder, Über die Auswirkungen der Ungleichverteilung des Wärmeübergangs am Rohrumfang bei der Verdampfung im durchströmten waagerechten Rohr, *Wärme- und Stoffübertragung* **13,** 265–274 (1980).
52. P. Palanikumar, The effect of tube inclination on heat transfer in the closed evaporative thermosyphon, M.S. thesis, University of Durham, England (1960).
53. S. S. Kutateladse, *Fundamentals of Heat Transfer*. E. Arnold, London, pp. 357–366 (1963).
54. G. D. Fulford, The flow of liquids in thin films, *Adv. chem. Engng* **5,** 151–236 (1964).
55. W. Nusselt, Die Oberflächenkondensation des Wasserdampfes, *Z. Ver. dt. Ing.* **60,** 541–546 and 569–575 (1916).
56. U. Grigull, Wärmeübertragung bei der Kondensation mit turbulenter Wasserhaut, *Forsch. Ing.-Wesen* **13,** 49–56 (1942) and *Z. Ver. dt. Ing.* **86,** 444–445 (1942).
57. K. E. Hassan and M. Jakob, Laminar film condensation of pure saturated vapours on inclined circular cylinders, ASME Paper No. 57-A-35.
58. W. Kamminga, An analytic solution of the film thickness of laminar film condensation on inclined pipes, *Int. J. Heat Mass Transfer* **23,** 1291–1293 (1980).
59. G. Selin, Heat transfer by condensing pure vapours outside tubes, *International Developments in Heat Transfer*. ASME, pp. 279–289 (1963).
60. T. W. Garrett and J. L. Wighton, The effect of inclination on the heat-transfer coefficient for film condensation of steam on an inclined cylinder, *Int. J. Heat Mass Transfer* **7,** 1235–1243 (1964).
61. R. L. Hirshburg, Laminar film flow phenomena—theory and application to the two-phase closed thermosyphon, Ph.D. thesis, Arizona State University (1980).
62. N. M. Stoyanov, Effect of the angle of inclination of a closed evaporative thermosyphon on heat transfer, *Teploénergetika* **15,** 74–76 (1968).

TRANSFERT THERMIQUE DANS UN THERMOSIPHON OPERANT AVEC UN FLUIDE PROCHE DE L'ETAT CRITIQUE

Résumé—On étudie expérimentalement le transfert thermique dans les zones de refroidissement et de réchauffement d'un thermosiphon fermé. On fait varier la pression du fluide ($0.8 \leqslant p/p_c \leqslant 1{,}0$), le flux thermique ($175 \leqslant \dot{Q} \leqslant 1975$ W) et l'angle d'inclinaison ($0 \leqslant \psi \leqslant 60°$). Le réfrigérant R 115 est utilisé comme fluide de travail. La quantité de fluide est déterminé en tenant compte du volume massique critique. L'ébullition apparait dans la zone de chauffage et la condensation dans la zone de refroidissement. Selon la pression, il y a trois régimes d'ébullition: ébullition nuclée, ébullition nuclée en régime de transition et l'ébullition en film. Dans le thermosiphon, il existe la condensation en film laminaire ou turbulent. Le transfert thermique couplé dans les zones de chauffage et de refroidissement cause un fonctionnement global avec des conditions optimales pour un angle d'inclinaison $\psi = 40°$ environ, un faible flux thermique et des pressions $0{,}9 < p/p_c < 1{,}0$, tant que l'ébullition en film n'apparait pas.

DER WÄRMEÜBERGANG IN EINEM ZWEI-PHASEN-THERMOSYPHON, DER EIN FLUID NAHE DEM THERMODYNAMISCH KRITISCHEN ZUSTAND ENTHÄLT

Zusammenfassung—Der Wärmeübergang in der Heiz- und Kühlzone eines geschlossenen Thermosyphons wird in Abhängigkeit von Fluiddruck ($0{,}8 \leqslant p/p_{krit} < 1{,}0$). Wärmestrom ($175 \leqslant \dot{Q} \leqslant 1975$ W) und Rohrneigung ($0 \leqslant \phi \leqslant 60°$) experimentell untersucht. Als Fluid dient das Kältemittel R 115. Die Füllmenge ist so bemessen, daß das mittlere spezifische Volumen den kritischen Wert annimmt. In der Heizzone findet Verdampfung statt, in der Kühlzone Kondensation. Bei der Verdampfung ergeben sich mit steigendem Druck drei Bereiche: Blasensieden, Blasensieden in einem Übergangsbereich, Filmsieden. Im Thermosyphon tritt teilweise laminare, teilweise turbulente Filmkondensation auf. Das Zusammenwirken der Vorgänge in der Heiz- und Kühlzone führt zu einem optimalen Gesamtverhalten bei einem Neigungswinkel $\phi = 40°$, kleinem Wärmestrom und bei Drücken $0{,}9 < p/p_{krit} < 1{,}0$, solange noch kein Filmsieden einsetzt.

ТЕПЛОПЕРЕНОС В ДВУХФАЗНОМ ТЕРМОСИФОНЕ, ЗАПОЛНЕННОМ ЖИДКОСТЬЮ В СОСТОЯНИИ, БЛИЗКОМ К КРИТИЧЕСКОМУ

Аннотация—Экспериментально изучен теплоперенос в зонах нагрева и охлаждения закрытого термосифона. Изменялись давление жидкости ($0{,}8 \leq p/p_c < 1{,}0$), скорость теплового потока ($175 \leq \dot{Q} \leq 1975$W) и угол наклона трубы ($0 \leq \varphi \leq 60$). В качестве рабочей жидкости применялся хладагент R115. Количество жидкости определялось по критическому удельному объему. Кипение имело место в зоне нагрева, а конденсация – в зоне охлаждения. Существует три режима кипения, зависящих от давления: пузырьковое, пузырьковое в переходном режиме и пленочное. В термосифоне наблюдаются ламинарная и турбулентная пленочные конденсации. Комбинированный теплоперенос в зонах нагрева и охлаждения обеспечивает общую производительность при оптимальных условиях (угол наклона $\varphi = 40$, малая скорость теплового потока, давление $0{,}9 < p/p_c < 1{,}0$) до момента возникновения пленочного кипения.